Journal of Structural Biology 203 (2018) 162–169

Contents lists available at ScienceDirect

Journal of Structural Biology

journal homepage: www.elsevier.com/locate/yjsbi

New zonal structure and transition of the membrane to mammillae in the eggshell of chicken *Gallus domesticus*

Yunong Li[a,b,*], Yang Li[c], Shirong Liu[a], Yang Tang[a], Bing Mo[c], Hui Liao[b]

[a] State Key Laboratory of Environmental Geochemistry, Institute of Geochemistry, Chinese Academy of Sciences, 99 Lincheng West Road, Guanshanhu District, Guiyang, Guizhou 550081, China

[b] Guiyang No.1 High School, 1 Xingzhu East Road, Guanshanhu District, Guiyang, Guizhou 550081, China

[c] Center of Lunar and Planetary Study, Institute of Geochemistry, Chinese Academy of Sciences, Guanshanhu District, Guiyang, Guizhou 550081, China

ARTICLE INFO

Keywords:
Amorphous calcium carbonate
Crystalline calcite
Eggshell structure
Avian egg
Chicken

ABSTRACT

Avian eggshell is a typical bio-engineered ceramics characterized by layer structures. These layers are categorized mainly by the form of crystalline calcite. Whether there exist other layer structures, how the membrane layer is transformed to the carbonate one, what form the carbonate takes after the transition. These questions remain to be clarified. Here we examine the eggshell of chicken *Gallus domesticus* by optical microscope, scanning electron microscope and transmission electron microscope. We find that there exists another layer structure defined by variation of organic matrices. The transition from the membrane to the mammillary cones is implemented through the calcium reserve assemblies or the mammillary cores. The integrity of the transitional structure was weakens as the reserved calcium is displaced, and loses completely in about 10 days of incubation. As the first deposited carbonate layer after the transition, the mammillary cones comprise amorphous calcium carbonate and clusters/assemblies of calcite crystallites the size about a nanometer, plus bubble pores extending preferentially in the lateral direction. Our results provide new insights into the structure and component of the avian eggshell, and may help decipher the constitution of the bio-ceramics in the perspective of material science.

1. Introduction

Avian eggshell is evolutionarily more advanced than that of reptiles in terms of structure and component (Hincke et al., 2012; Ola et al., 2012). Deposited from the inside out, it is characterized by various layers. The innermost is the membrane layer. It is composed of a network of fibers made of multiple kinds of proteins (Wedral et al., 1974). Outside the membrane layer covers the true shell (Ketta and Tumova, 2016). It comprises the layers of calcium carbonate, the only mineral constituent of the shell (Nys et al., 1991), as well as the cuticle. The carbonate layer is 94–97% of calcite (Cain and Heyn, 1964) associated with organic matrices (Chien et al., 2009b; Chien et al., 2008; Gautron et al., 1997). It is further divided into the mammillary layer, palisade layer and vertical crystal layer by the form of crystalline calcite (Perrott et al., 1981). The mammillary layer is a regular array of cones or knobs that are reportedly comprised of crystalline calcite (Bunk and Balloun, 1977; Rodriguez-Navarro et al., 2015) without preferred orientation (Bunk and Balloun, 1977). Each cone or knob has in the top a core of calcium carbonate and concentrated organic matter (Cusack et al., 2003), or a calcium reserve assembly that contains microcrystals of calcite (Chien et al., 2009b; Deickert et al., 1989; Dennis et al., 1996). This layer covers directly on the membrane layer and is involved in the most dramatic transition of layers in the eggshell (Hincke et al., 2012). The palisade layer consists of calcite crystals without significant preferred orientation (Perrott et al., 1981) but with large quantities of air conducting pores (Ketta and Tumova, 2016; Solomon, 2010). These pores are classified by size as “gas pores” in micro-scale, “bubble pores” in submicro-scale, and even smaller pores in nano-scale (Zhou et al., 2011). The vertical crystal layer, also known as the surface crystal layer, comprises highly orientated calcite. The cuticle layer is primarily an organic layer with small amounts of needlelike hydroxyapatite (Dennis et al., 1996). This layer is very thin and often patchy or even missing in the outer surface of eggshell (Kusuda et al., 2011; Samiullah and Roberts, 2014). The complicated layer structure and transition of the membrane layer to the carbonate one partly distinguished the avian eggshell from majority of reptiles’ (Hincke et al., 2012). The layer structure, however, was divided mainly by the form of crystalline calcite (Garcia-Ruiz et al., 1995; Nys et al., 2004). Whether there exist other forms of structure, how the membrane layer was transformed into the carbonate one, what form the carbonate takes after the transition,

* Corresponding author at: State Key Laboratory of Environmental Geochemistry, Institute of Geochemistry, Chinese Academy of Sciences, 99 Lincheng West Road, Guanshanhu District, Guiyang, Guizhou 550081, China.
E-mail address: miaomiaoCSNS@hotmail.com (Y. Li).

https://doi.org/10.1016/j.jsb.2018.04.006
Received 26 November 2017; Received in revised form 26 April 2018; Accepted 28 April 2018
Available online 30 April 2018

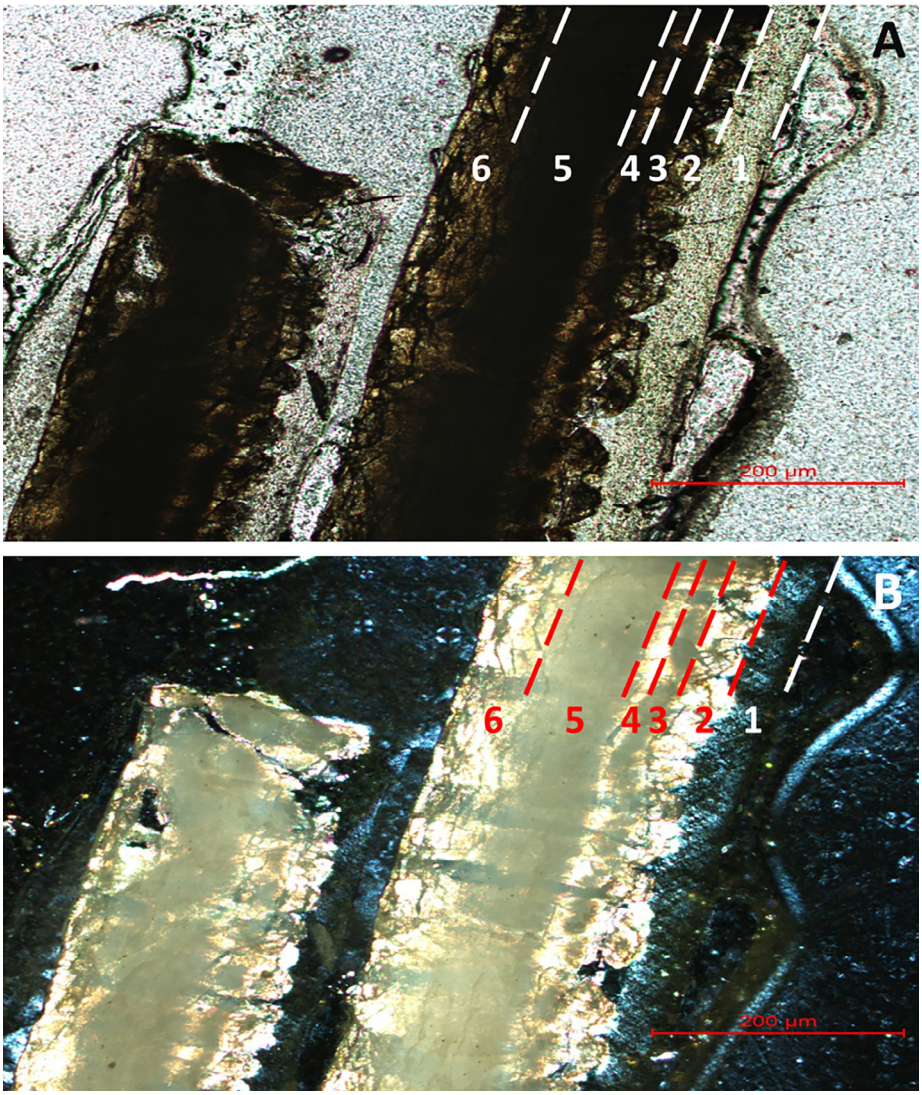

Fig. 1. The new zonal structure revealed by the optical microscope of the eggshell at day 0 (right) and day 5 (left) of incubation. (A) Polar light, (B) cross-polar light. The dashed lines demarcate the layers, the digits mark the layer.

and how the transitional structure changes during incubation. These questions remain to be clarified despite the studies in the past decades. They are important for understanding the evolutionary trait of avian eggshell, as well as for comprehending the structure and component of the bio-engineered ceramics as a material.

2. Materials and methods

2.1. Material

The eggs used in the experiment were laid by *Gallus Domesticus*, a subspecies of domestic chicken commonly raised in the mountainous area in Guizhou province, southwest China. They were incubated in an Aida FCMICS incubator and sampled at day 0 (unincubated egg), 5, 10, 15 and 21 of incubation. The eggshell was separated from the embryo manually and air-dried for sample preparation.

2.2. Preparation of thin slices

Eggshells were glued together in the order of incubation days, with the inner surface facing the same direction. These grouped eggshells were first impregnated with glue and then cut in cross-section to make thin slices about 3 μm thick by the standard procedures of rock slice preparation in petrological studies.

2.3. Preparation of ultra-thin slices

Ultra-thin slices of unincubated eggshell were prepared by the ion-beam thinning technique. The preparation was done by the FEI Scios Dual beam. The sections were dug in the middle of a mammillary cone using ion beam of 15 nA, and then milled into slices less than 100 nm thick by the ion beam of 3 nA. The slice thinning was made by the ion beams transmitted vertically from upside down. Both the digging and milling were done at the voltage of 30 kV. The upper edge of the ultra-thin slices was strengthened by a bar of Pt about 2 μm wide. It was deposited using Ga^+ beam at 300 pA and 30 kV. The made slices were attached on copper grids and ready for electron microscopic studies.

2.4. Optical microscopic observations

Optical microscopic observation of the slices was performed by a Leica DM2700P optical microscope. Photographs were taken and recorded by a computer connected to the microscope.

2.5. Scanning electron microscopic (SEM) observations

The eggshells in different incubation days were installed onto a baseplate using conductive resins and coated with carbon. They were investigated by a JSM-6460LV Scanning Electron Microscope. Elemental compositions of the eggshells were analyzed by the energy spectrometer attached to the microscope.

2.6. Transmission electron microscopic (TEM) observations

The ultra-thin slices were observed by a Tecnai G2 F20 S-TWIN TMP Transmission Electron Microscope. The techniques employed include the high magnification bright field topography imaging analysis, high resolution lattice imaging analysis, selected area electron diffraction (SAED) analysis and Fourier transform structural analysis. The accelerating voltage was 200KV, the magnification was between 3000 and 300,000 times.

3. Results

3.1. Layer structure under optical microscope

The unincubated eggshell shows six layers of different light transmittance under optical microscope (Fig. 1), suggesting different constitution between the layers. To the left of the unincubated eggshell is the one that has been incubated for 5 days. It shows the same layers as the unincubated one. Some of the layers are coincidental with the previous ones, others not. From right to left of the shell, the first layer is about 45 μm thick, transparent in polar light and opaque in cross-polarized light, clearly different to the rest of the eggshell in terms of transparency under both polar and cross light. This layer is exactly the membrane layer. The second layer is about 35 μm, translucent in polar light and transparent in cross light. It matches the mammillary cone layer. The third layer is opaque in both polar and cross light, approximately 33 μm thick and somewhat wavy or discontinuous in the lateral direction. The fourth layer is around 15 μm thick and similar to the second layer in the light transmittance. The fifth layer is about 60 μm thick and similar to the third layer in the light transmittance. The sixth layer is about 60 μm, translucent in polar light and transparent in cross light. The third-fifth layers are included in the palisade layer while the sixth layer covers part of the palisade layer, the whole vertical crystal layer and the cuticle layer.

3.2. Structures connecting the membrane and mammillary cones

SEM observations show that the fibers of the outer shell membrane end on a structure that looks rough on surface. The structure is located on top of the mammillary knob with a smaller diameter about 30 μm in average. The rough surface and the situation make the structure look like a flower bud in the stage of incipient opening on the tip of a cone (Fig. 2A). We therefore named it the bud-like structure in this study. A close-up view shows that the fibers seemingly penetrate into the bud (Fig. 2B), which is in agreement with the early report (Bunk and Balloun, 1977), but the appearance on the opposite side of the structure indicates that it is better to be described as “end on” because the bud-like structure appears to be stuck on the surface of the membrane (Fig. 2C), and no trace of fibers is detected in the inner side of the bud-like material (Fig. 2D), nor found in the mammillary cones (Fig. 2E, F). Compositional variation along the fiber indicates that the organic-rich fiber is substituted for carbonate as it reaches the bud-like structure. As shown by the results of energy spectra analyses, both S/Ca and C/O decline as the fibers extends to the bud-like structure (Fig. 3). S/Ca reduces from 0.12 to 0.08 at point 1 and 2, respectively, and becomes negligibly small at point 3. Correspondingly, C/O decreases from 4.02 to 2.00 and then to 0.66. Sulphur is an important element in proteins and sulfated proteoglycans, which are rich in the membrane fibers (Rodriguez-Navarro et al., 2015), and calcium the main element of calcium carbonate. S/Ca indicates the content of organic matter relative to calcium carbonate. The decreased S/Ca suggests that organic matter decreases relative to calcium carbonate. C and O are both major elements in organic matter and calcium carbonate, yet C/O is higher in organic matter than in calcium carbonate. The decreased C/O confirms that organic matter decreases relative to calcium carbonate as the fiber grows closer to the mammillary cones. Point 3 is located on the surface of the bud, the elemental composition indicates that it is composed primarily of carbonate. Therefore, when the fiber reaches the bud-like structure, deposition of carbonate takes place.

The transition of the fiber to the bud-like structure proves that the mammillary knobs were deposited on distinct site on the outer shell membrane (Rodriguez-Navarro et al., 2015). Thanks to this connection, the membrane layer is firmly attached to the mammillary cones and difficult to be separated mechanically. However, the attachment weakens in incubation, becoming partly detached at day 5 and completely detached at day 10 (Fig. 4). Microscopic pictures of the cross-section of two sets of the eggshells that were placed in the order of incubation days (Fig. 4A) manifests that the membrane layer attaches on the mammillary cones at day 0 and 5 (Fig. 4B, C), displaying a smooth inner edge in the cross section and also differing in color to the mammillary cones and the other carbonate layers under the polarized light. However, the cross sections are free of the membrane layer at day 10, showing a rough inner margin indicative of the mammillary cones (Fig. 4B, C). SEM images of cross sections of the eggshells also reveal that the membrane is attached to the shell at day 0 (Fig. 4D), but begins to separate from some mammillary cones at day 5 (Fig. 4E), and becomes completely detached at day 10 and 15 (Fig. 4F, G). The complete detachment of the membrane layer was also evidenced in the removal of the embryo from the eggshell during sample preparation. The embryo was wrapped completely by the membrane at day 10 after taken out of the shell, while being exposed at day 5 just as it is taken out from an unincubated egg. In the latter two cases, the membrane remained stuck on the inner shell rather than wrapping the embryo. The detachment occurs between the bud-like structure and the knob with the bud still attached to the outer membrane (Fig. 2C, D), exposing the pit in the top of mammillary cones (Fig. 2E, F).

3.3. Air pores in the mammillary layer

The two ultra-thin slices were cut with one’s plane facing about vertically (Fig. 5A) while the other’s about laterally (Fig. 5B) in the shell. Both slices are perforated (Fig. 5C, D), indicating the air pores in the mammillae (Solomon, 2010). The holes are basically circular given that they were deformed elliptically in the vertical direction by the bombardment of the ion beams during the slice thinning. The diameter in the horizontal direction ranges from 0.12 – 0.37 μm and 0.12 – 0.43 μm in the slice C and D, respectively, all belonging to the bubble pores. These pores are supposedly used for adjustment of air conduction (Zhou et al., 2011). Some of them, however, do not penetrate through but rather end in the slice. They may represent voids without outlets, or air channels in zigzags with these pores as the turning point. Despite this uncertainty, the original circular shape suggests that the air channels are about perpendicular to the slices. By the direction of the two slices, we infer that the pores extend not only from the inside out, but also in the lateral direction. The latter is quite contrary to the common sense because the pores are supposed to exchange air and moisture with the outside environment. The holes in the slice C are approximately half as many as in D, suggesting that more pores extend laterally than vertically in the mammillary layer.

3.4. Texture of the calcium carbonate in the mammillary cones

TEM observation of the ultra-thin slices show that calcium carbonate in the mammillary cones are in two kinds of texture. One is fine

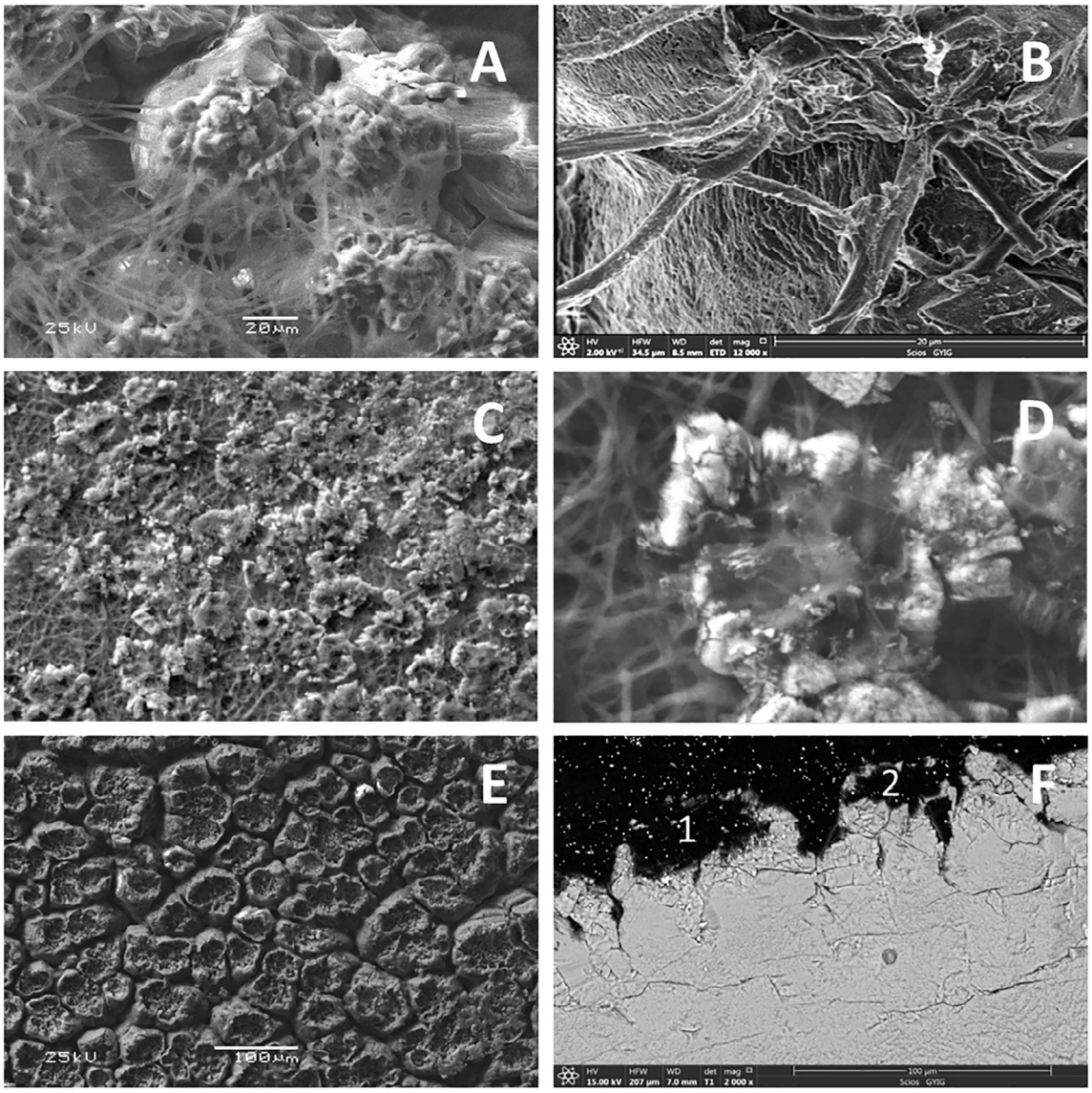

Fig. 2. SEM images showing the connection of the membrane fibers to the mammillary cones at day 0 (A, B) and their complete detachment at day 21 of incubation (C-F). (C) Opposite view of the bud-like structure stuck on the outer membrane after complete detachment, showing clearly that the membrane has no connection with the mammillary cones except through the bud-like structure. (D) Enlarged opposite view of the bud-like structure. (E) Pits left in the tip of mammillary cones after complete detachment of the membrane layer. (F) Cross section view of the mammillary cones, digits 1 and 2 indicate two pits left in top of the cones.

and homogeneous that looks like even areas, the other appears as rough patches or loose assembly of rough grains the size about a nanometer or even smaller (Fig. 6A). Close-up observations indicate that the rough patches seem like rocky mountains protruding out of the smooth plain (fine texture) (Fig. 6B). Electron bombardment and SAED reveal that the fine texture is constituted by amorphous calcium carbonate (ACC) while the rough texture by polycrystalline calcite. At irradiation of the electron beam, the image in B was changed successively in every minute into that in C and D. The fine texture was transformed quickly into the rough one, occurring preferentially from the periphery of the rough patches (Fig. 6B-D), suggesting that ACC was crystallized progressively into the calcite, and that the existing crystallites provided favorable sites for the crystallization. SAED analysis of the smooth area reveals no diffraction pattern of the polycrystalline calcite, which is characterized by circles of different radius (Cain and Heyn, 1964), but only a few pairs of faint dots symmetric about the center (Fig. 6E). It suggests that only minute single calcite crystallite was bumped by the electron beam in the selected area. This is in agreement with what was observed in panel A. After one minute of electron bombardment, one pair of faint dots grew stronger while two weak circles began to appear in the four corners of the SAED image (Fig. 6F). Apparently, the single crystallite in the selected area grew larger through crystallization, meanwhile, more minute crystallites took place from the ACC in the area, giving rise to the faint circles of diffraction. After one more minute of bombardment, the diffraction circles became stronger (Fig. 6G), suggesting that the crystallites generated a minute ago grew larger. These SAED results are consistent with those of TEM observations very well (Fig. 6B-D).

4. Discussions

4.1. Uneven distribution of organic matrices in the true shell

The layered structure is the most typical feature in the avian eggshell (Hincke et al., 2012). Except the membrane layer whose flexibility makes it easily recognizable, the true shell is divided by the structure of crystalline calcite as a result of competitive growth in the shell deposition (Perrott et al., 1981). As minor constituents that account for

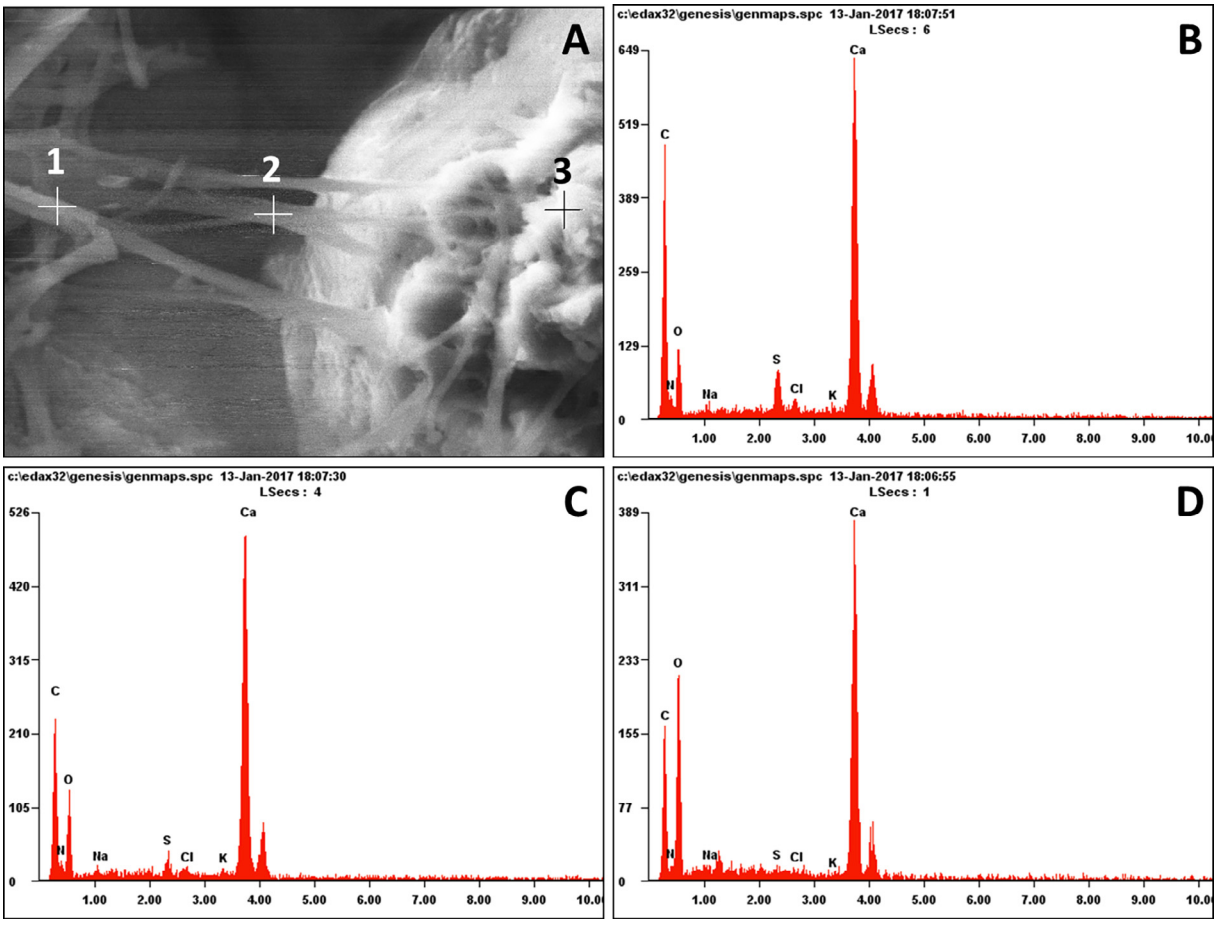

Fig. 3. SEM image of the membrane fibers and a connected cone in a day 0 shell and the result of energy spectra analysis. (A) Location of the analytical points. (B), (C) and (D) The analytical result for point 1, 2 and 3, respectively.

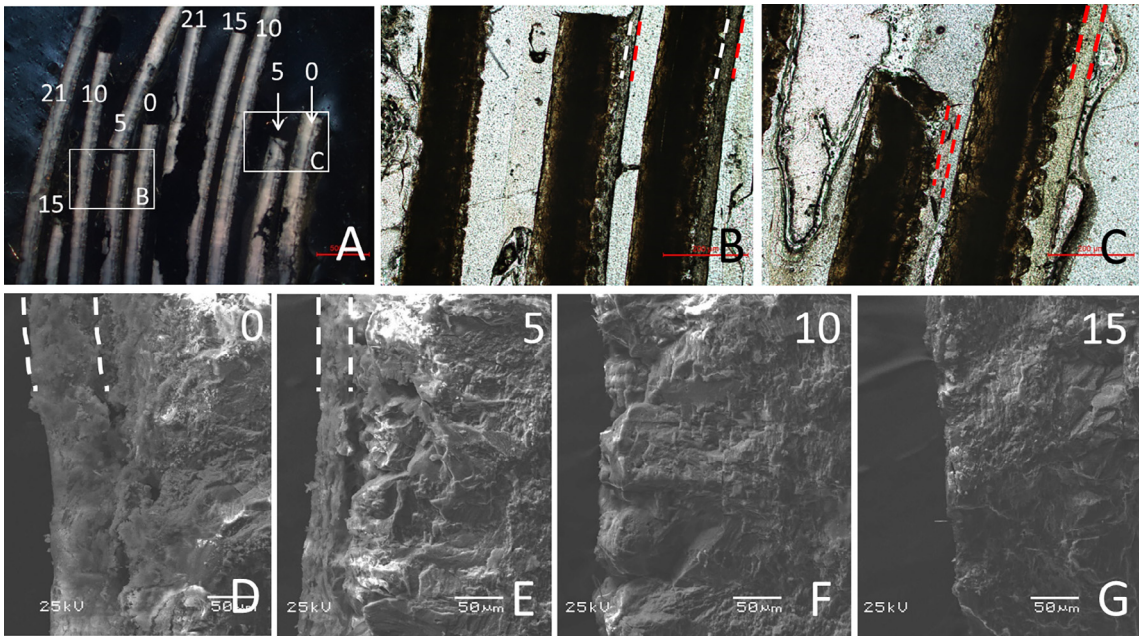

Fig. 4. Microscopic (A-C) and SEM (D-F) images indicating the complete detachment of the membrane layer at day 10 of incubation in comparison to day 0 and 5. The digits represent the days of incubation. The rectangles in A are the areas magnified in B and C. The dash lines indicate the membrane layer.

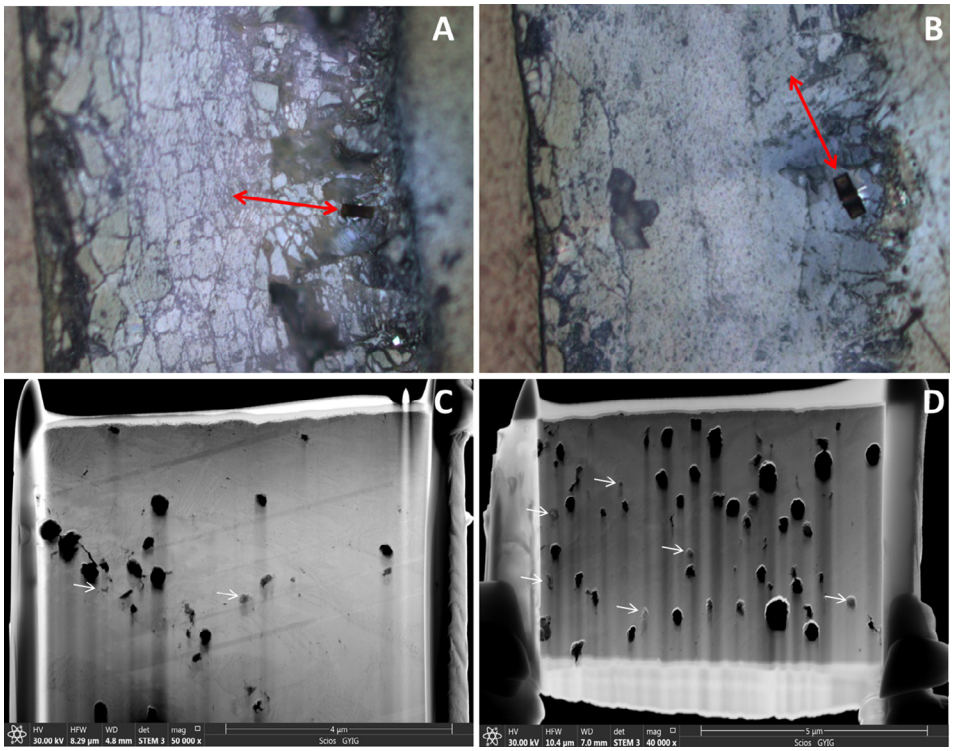

Fig. 5. Reflected-light microscopic images of the unincubated eggshell (A, B) and the SEM images of the ultra-thin slices (C, D). The black solid rectangles in (A) and (B) are the areas dug for the slice manufacture. The slice C was cut from the rectangle in (A), and the slice D from the rectangle in (B). The bidirectional arrows in (A) and (B) indicate the directions the ultra-thin slice is facing, the white single direction arrows in (C) and (D) point to the pores not penetrating through the slice.

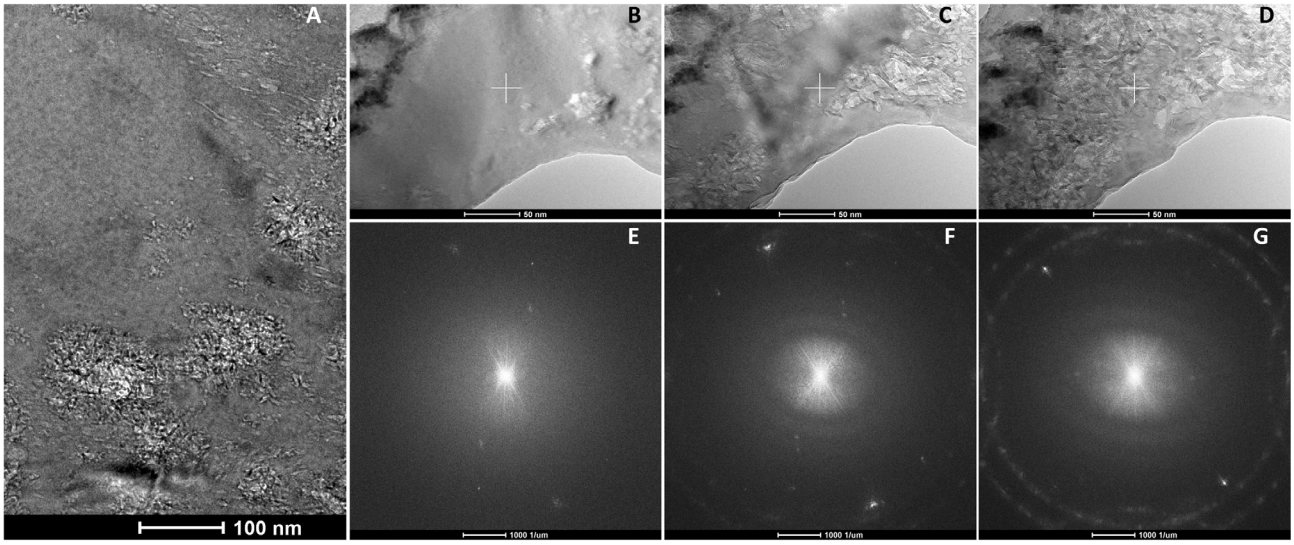

Fig. 6. TEM images of the ultra-thin slices (A-D) and the results of SAED analysis (E-G). (A) Fine texture (smooth area) of amorphous calcium carbonate and rough texture of clusters of calcite crystallites. (B) Close-up observation of the amorphous calcium carbonate and the crystalline calcite near a bubble pore. (C, D) Progressive crystallization of amorphous calcium carbonate under electron bombardment. (E-G) SAED graph in B, C and D, respectively, revealing the increased crystallization under the electron irradiation. The cross in (B-D) indicate the center of the SAED analysis.

only a few percent in the true shell (Cain and Heyn, 1964), organic matrices, which are mainly matrix proteins, glycoproteins and proteoglycans (Chien et al., 2009b; Chien et al., 2008), play no role in the previous division of the layers. This study found a layer structure defined by variation of the organic matrices, characterized by different transmittance of light under optical microscope. The layers with low organic matrices have high light transmittance while those of high organic matrices appear opaque or translucent. The true shell is deposited in hen's uterus, where the uterine fluid contains various organic matrices (Brionne et al., 2014; Gautron et al., 1997), as well as calcium and bicarbonate that are supersaturated with respect to calcite (Nys et al., 1999) or ACC as reported recently (Rodriguez-Navarro et al., 2015). Consequently, the organic matrices pervade the true shell as soluble and insoluble fractions (Nys et al., 1999). The new layer structure reveals that the organic matrices are not distributed homogeneously in the true shell but concentrated in two zones in the palisade layer. Deposition of the true shell takes about 17 h (Hincke et al., 2012), a particular profile of specific proteins is present in the uterine fluid at different stage of the deposition (Gautron et al., 1997; Rodriguez-Navarro et al., 2015). The variation of proteins might result in the new zonal structure.

4.2. Transition from the membrane to mammillae

The change from the layer of membrane to the mammillae is the most dramatic one in the chicken eggshell as the two layers are distinct in structure and components. Two sets of terminology were invented in the past decades to describe the structures relevant, but neither took them as the transition between the two layers. One terminology is "the mammillary core", the other "calcium reserve assembly". The former indicates a rounded organic-rich structure that forms directly in the surface of the outer membrane (Bunk and Balloun, 1977). Calcium carbonate deposits first on the outer rim of the core, from whence originates the mammillary knob followed by other layers of the true shell (Robinson and King, 1963; Robinson and King, 1968; Rodriguez-Navarro et al., 2015; Simkiss and Tyler, 1957). This terminology was invented from the perspective of eggshell mineralization. The calcium reserve assembly is composed of a baseplate, a calcium reserve body and a cover (Chien et al., 2009b; Deickert et al., 1989; Dennis et al., 1996). The baseplate is composed of ACC (Rodriguez-Navarro et al., 2015) deposited directly in the surface of outer membrane (Deickert et al., 1989; Dennis et al., 1996). It is shaped like a disc with a flat top surface (Rodriguez-Navarro et al., 2015). The calcium reserve body is like a sac (Chien et al., 2008; Dennis et al., 1996), containing microcrystals of calcite (Dennis et al., 1996; Nys et al., 2004) or organic matrix plus possible ACC (Chien et al., 2009b). These components are dissolved during incubation to nourish the embryo (Chien et al., 2009b; Hincke et al., 2012). The calcium reserve assembly was coined to understand calcium reserve and provision for embryo development. Both terminologies take the structures as an integral part of the mammillary knob. However, we believe it would help tackle the structural development of avian eggshell if the structures are taken as the transition from the membrane to the mammillae. This is supported by their role in connection/separation of the membrane to mammillae, as well as their change in incubation. The bud-like structure was the appearance of the baseplate viewed from the bottom in contrast to the flat surface on top (Rodriguez-Navarro et al., 2015). The fibers of the outer membrane end on the bottom of the baseplate with the dominant component changing gradually from organic matter to calcium carbonate. This transition makes the baseplate firmly connected to the outer membrane in any circumstances, including incubation. It serves as a lid over the pit in the top of the mammillary cone. Inside the space is located the organic-rich component of the core or the calcium reserve body sac (Deickert et al., 1989). The pit is formed when calcium carbonate was deposited around the organic core (Rodriguez-Navarro et al., 2015). Both the baseplate and the calcium reserve sac are pivotal in the transition. Through these structures, the membrane layer is replaced by the true shell with tight yet maneuverable connections. The fastening of the baseplate with the membrane makes the latter a liner on the rough surface of mammillae, creating a smooth surround for the embryo while strengthening the physical intensity of the true shell. The calcium body sac reserves the nutrient while helping with the fastening. During incubation, however, the calcium reserve or the organic core is consumed (Holm et al., 2013; Karlsson and Lilja, 2008), weakening the connection centrally between the baseplate and the mammillary cone. Once the reserve is absent, the membrane layer is ready to be disconnected to the true shell, facilitating the chick hatching (Chien et al., 2009a,b). Calcium reserve/consumption is associated with shell strengthening/weakening in such an amazing way that it serves as a paradigm of evolution.

The strength of the connection between the membrane and the mammilla indicates the state of the calcium reserve consumption. Exposure of the pit in top of mammillary cone is a result of complete consumption of the calcium reserve (Chien et al., 2009b). We found that the membrane peeled off readily at day 10 of incubation, exposing the crater-like structure as shown in Fig. 2E-F. This period of time is about 6 days shorter than the reported ultimate loss of the reserve in case of White Leghorn chickens (*Gallus gallus*) (Chien et al., 2009b). It suggests that displacement of the calcium reserve took place in the early stage of incubation. This contradicts, however, the long held notion that the reserve was consumed at the late stage of embryo development, starting from about day 12–14 of incubation (Johnston and Comar, 1955; Tuan, 1980). One plausible explanation is that translocation of the calcium reserve happens in the early stage of incubation. The calcium, however, is not nourishing the developing embryo directly but stored in the yolk via the chorioallantoic membrane (Tuan, 1980), an organ important for Ca^{2+} transportation between the shell and the embryo (Moran, 2007; Terepka et al., 1976), it is not consumed until the late stage of incubation when the original yolk calcium was exhausted.

4.3. ACC and crystalline calcite after the transition

The mammillary cones were reportedly comprised of crystalline calcite (Chien et al., 2009a,b; Deickert et al., 1989; Dennis et al., 1996; Hincke et al., 2012; Nys et al., 2004; Reyes-Grajeda et al., 2004), suggesting that, once the transition is completed, the mineral calcite begins to dominate the eggshell as the major component. Compared to the rest layers of the true shell, calcite in the mammillary cones are believed to be in the form of crystallites in random orientation (Cain and Heyn, 1964; Perrott et al., 1981). Mineralization experiment also showed that crystalline calcite was ready to form on the periphery of the calcium reserve assemblies (Wu et al., 1995). A most recent study further indicated that ACC was ready to be deposited around the mammillary cores due to its equilibrium with the uterine fluid, but it was soon converted into crystalline calcite (Rodriguez-Navarro et al., 2015). In this mechanism, calcite crystals radiate from the mammillary cores and continue growing outwards to give rise to the true shell (Rodriguez-Navarro et al., 2015). Up to now, no report has been found to support the existence of ACC in the mature mammillary cones. Our own optical microscopic observations also showed crystalline features of calcium carbonate under cross-polarized light (Fig. 1B). However, our TEM observation revealed that the mammillary cones were composed of ACC and clusters of calcite crystallites. Although we did not analyse the ACC directly, we are certain about its amorphous form because it shows no apparent crystal structure under TEM. We inferred its carbonate composition based on three facts: 1) no other composition has ever been found in the true shell except carbonate; 2) it was transformed into calcite without adding any other composition, suggesting the composition is the same as calcite; and 3) the quick crystallization at the periphery of crystalline calcite proves the amorphous substance as carbonate. Clusters or assemblies of calcite crystallites are distributed in the ACC, making the mammillary cones look like crystalline under optical microscope. They can be discerned, however, after the resolution is magnified over 20,000 times in TEM observations.

Acknowledgements

This study is financially supported by the opening fund of the State Key Laboratory of Environmental Geochemistry (SKLEG2016905). The Institute of Geochemistry kindly allowed the first author to use the scientific instruments at the assistance of the co-authors. The first author thanks Mr. Fujun Jia in Guiyang No.1 High School for support of this research. As a class counselor, he gave the first author flexible time to perform the experiments and write the manuscript. Professor Xinqing Lee in the Institute of Geochemistry advised on the experiments and revised the manuscript. Constructive comments of the two anonymous reviewers contributed to the paper's revision. Their time and efforts were fully appreciated by the authors.

References

Brionne, A., Nys, Y., Hennequetantier, C., Gautron, J., 2014. Hen uterine gene expression profiling during eggshell formation reveals putative proteins involved in the supply of minerals or in the shell mineralization process. BMC Genomics 15, 220.

Bunk, M.J., Balloun, S.L., 1977. Structure and relationship of the mammillary core to membrane fibres and initial calcification of the avian Egg Shell. Br. Poult. Sci. 18, 617–621.
Cain, C.J., Heyn, A.N.J., 1964. X-ray diffraction studies of crystalline structure of avian egg shell. Biophys. J. 4, 23–39.
Chien, Y.C., Hincke, M.T., McKee, M.D., 2009a. Avian eggshell structure and osteopontin. Cells Tissues Organs 189, 38–43.
Chien, Y.C., Hincke, M.T., McKee, M.D., 2009b. Ultrastructure of avian eggshell during resorption following egg fertilization. J. Struct. Biol. 168, 527–538.
Chien, Y.C., Hincke, M.T., Vali, H., McKee, M.D., 2008. Ultrastructural matrix-mineral relationships in avian eggshell, and effects of osteopontin on calcite growth in vitro. J. Struct. Biol. 163, 84–99.
Cusack, M., Fraser, A.C., Stachel, T., 2003. Magnesium and phosphorus distribution in the avian eggshell. Comp. Biochem. Physiol. B: Biochem. Mol. Biol. 134, 63–69.
Deickert, J.W., Dieckert, M.C., Creger, C.R., 1989. Calcium reserve assembly: a basic structural unit of the calcium reserve system of the hen egg shell. Poult. Sci. 68, 1569–1584.
Dennis, J.E., Xiao, S.Q., Agarwal, M., Fink, D.J., Heuer, A.H., Caplan, A.I., 1996. Microstructure of matrix and mineral components of eggshells from white leghorn chickens (*Gallus gallus*). J. Morphol. 228, 287–306.
Garcia-Ruiz, J.M., Navarro, A.R., Kalin, O., 1995. Textural analysis of eggshells. Mater. Sci. Eng., C 3, 95–100.
Gautron, J., Hincke, M.T., Nys, Y., 1997. Precursor matrix proteins in the uterine fluid change with stages of eggshell formation in hens. Connect. Tissue Res. 36, 195–210.
Hincke, M.T., Nys, Y., Gautron, J., Mann, K., Rodriguez-Navarro, A.B., McKee, M.D., 2012. The eggshell: structure, composition and mineralization. Front. Biosci. Landmark 17, 1266–1280.
Holm, L., Österström, O., Lilja, C., 2013. Calcium mobilization from the avian eggshell during embryonic development. Anim. Biol. 63, 33–46.
Johnston, P.M., Comar, C.L., 1955. Distribution and contribution of calcium from the albumin, yolk and shell to the developing chick embryo. Am. J. Physiol. 183, 365–370.
Karlsson, O., Lilja, C., 2008. Eggshell structure, mode of development and growth rate in birds. Zoology 111, 494–502.
Ketta, M., Tumova, E., 2016. Eggshell structure, measurements, and quality-affecting factors in laying hens: a review. Czech J. Anim. Sci. 61, 299–309.
Kusuda, S., Iwasawa, A., Doi, O., Ohya, Y., Yoshizaki, N., 2011. Diversity of the cuticle layer of avian eggshells. J. Poultry Sci. 48, 119–124.
Moran, J.E.T., 2007. Nutrition of the developing embryo and hatchling. Poult. Sci. 86, 1043–1049.
Nys, Y., Zawadzki, J., Gautron, J., Mills, A.D., 1991. Whitening of brown-shelled eggs: mineral composition of uterine fluid and rate of protoporphyrin deposition. Poult. Sci. 70, 1236–1245.
Nys, Y., Gautron, J., Garcia-Ruiz, J.M., Hincke, M.T., 2004. Avian eggshell mineralization: biochemical and functional characterization of matrix proteins. Comptes Rendus – Palevol 3, 549–562.
Nys, Y., Hincke, M.T., Arias, J.L., Garcia-Ruiz, J.M., Solomon, S.E., 1999. Avian eggshell mineralization. Poultry Avian Biol. Rev. 10, 143–166.
Ola, O., Sterström, Clas, L., 2012. Evolution of avian eggshell structure. J. Morphol. 273, 241–247.
Perrott, H.R., Scott, V.D., Board, R.G., 1981. Crystal orientation in the shell of the domestic fowl: an electron diffraction study. Calcif. Tissue Int. 33, 119–124.
Reyes-Grajeda, J.P., Moreno, A., Romero, A., 2004. Crystal structure of ovocleidin-17, a major protein of the calcified Gallus gallus eggshell – implications in the calcite mineral growth pattern. J. Biol. Chem. 279, 40876–40881.
Robinson, D.S., King, N.R., 1963. Carbonic anhydrase and formation of the hen's egg shell. Nature 199, 497–498.
Robinson, D.S., King, N.R., 1968. Mucopolysaccharides of an avian egg shell membrane. J. R. Microscopical Soc. 88, 13–22.
Rodriguez-Navarro, A.B., Marie, P., Nys, Y., Hincke, M.T., Gautron, J., 2015. Amorphous calcium carbonate controls avian eggshell mineralization: a new paradigm for understanding rapid eggshell calcification. J. Struct. Biol. 190, 291–303.
Samiullah, S., Roberts, J.R., 2014. The eggshell cuticle of the laying hen. Worlds Poultry Sci. J. 70, 693–707.
Simkiss, K., Tyler, C., 1957. A histochemical study of the organic matrix of hen egg-shells. Q. J. Microsc. Sci. 98, 19–28.
Solomon, S.E., 2010. The eggshell: strength, structure and function. Br. Poultry Sci. 51, 52–59.
Terepka, A.R., Coleman, J.R., Armbrecht, H.J., Gunter, T., 1976. Transcellular transport of calcium. Symp. Soc. Exp. Biol. 30, 117–140.
Tuan, R.S., 1980. Calcium transport and related functions in the chorioallantoic membrane of cultured shell-less chick embryos. Dev. Biol. 74, 196–204.
Wedral, E.M., Vadehra, D.V., Baker, R.C., 1974. Chemical composition of cuticle, and inner and outer shell membranes from eggs of *gallus-gallus*. Comp. Biochem. Physiol. 47, 631–640.
Wu, T.-M., Rodriguez, J.P., Fink, D.J., Carrino, D.A., Blackwell, J., Caplan, A.I., Heuer, A.H., 1995. Crystallization studies on avian eggshell membranes: implications for the molecular factors controlling eggshell formation. Matrix Biol. 14, 507–513.
Zhou, J., Wang, S., Nie, F., Feng, L., Zhu, G., Jiang, L., 2011. Elaborate architecture of the hierarchical hen's eggshell. Nano Res. 4, 171–179.